Scripta Materialia xxx (2015) xxx–xxx

Contents lists available at ScienceDirect

Scripta Materialia

journal homepage: www.elsevier.com/locate/smm

Tailored metal–ceramic nanocomposites prepared by redox cycling of polycrystalline Ni-doped yttria stabilized zirconia

Amy Morrissey [a], James R. O'Brien [b], Ivar E. Reimanis [a,*]

[a] Colorado Center for Advanced Ceramics, Metallurgical and Materials Engineering Department, Colorado School of Mines, Golden, CO 80401, USA
[b] Off Grid Research, 6501 Goodwin Street, San Diego, CA 92111, USA

ARTICLE INFO

Article history:
Received 14 August 2015
Accepted 15 September 2015
Available online xxxx

Keywords:
Nanocomposite
Oxidation
Magnetic properties
Ni-YSZ

ABSTRACT

We demonstrate it possible to tailor unique metal–ceramic nanocomposites through redox cycling of Y_2O_3-stabilized ZrO_2 containing 0.5 molar percent NiO (below the solubility limit). Upon the first reduction, Ni^{2+} ions precipitate as metallic Ni^0 at pores, grain boundaries, or within the grain interiors with specific size ranges (~5 nm/~30 nm/~200 nm) for each. Upon oxidation, Ni^{2+} ions form, but their distribution is not the same as the original microstructure. In particular, NiO forms, and subsequent reduction leads to a distribution of metallic Ni different from that in the first reduction. One can ratchet the dissolution/precipitation behavior to form particular nanoscale arrangements.

Nanocomposite oxides containing dispersed metallic or metal–oxide nanoparticles offer improved structural and/or energy-related properties compared with monolithic oxides [1]. The high interfacial area may lead to space charge layers that enhance the mass transport of charged species [2,3] and may be designed for use in electroceramic devices and sensors [4–7]. It is generally challenging to engineer stable metal–ceramic nanocomposites due to thermodynamic and kinetic instabilities at the nanoscale [5].

Internal reduction has previously been considered as a method to make nanoscale Ni-YSZ composites [8]. Ni^{2+} ions dissolved in the YSZ lattice may be exsolved in a reducing atmosphere to form metallic Ni^0. The YSZ microstructure plays an important role in the size and distribution of Ni^0. In particular, microstructural features such as grain boundaries and porosity may be sites for fast transport pathways and may be preferential sites for Ni^{2+} ions and/or metallic Ni^0 [9–11]. Space charge effects also would be expected to play a role [12,13].

The reduction–oxidation behavior of nickel-doped YSZ has been widely studied in context of solid oxide fuel cell (SOFC) anodes [14–19]. Typically, Ni contents up to about 40 molar % are used, leading to an interconnected Ni-porous-YSZ microstructure with a high density of triple point boundary reaction sites [20–22]. The direct reduction and direct oxidation are of interest not only in SOFC anode fabrication, but in operation. In the present work, a composition of 0.5 molar percent NiO dopant is chosen since it is well below the solubility limit [23,24], thereby facilitating a study to examine the exsolution and dissolution of Ni^{2+} ions in YSZ. Previous studies on the redox behavior of Ni-YSZ have not been performed for levels below the solubility limit.

The specimens were prepared by high purity chemical synthesis described elsewhere [25]. The redox cycles were conducted in a dedicated furnace [26]. It was shown that all nickel exists as randomly distributed Ni^{2+} ions and that no NiO is present [26]. Reduction was performed at 1000 °C for 25 h flowing in H_2 gas (2% H_2/Ar balance). Oxidation was performed at 1000 °C for 25 h in flowing synthetic air (21% O_2/Ar balance). A temperature of 1000 °C was selected because it is below the temperature where grain growth occurs [27]. All heating and cooling was performed in flowing Ar gas. After the first reduction step metallic Ni^0 forms in a manner that is highly dependent on the YSZ microstructure. A distribution of Ni^0 size is observed: ~200 nm within pores, ~20 nm along grain boundaries, and ~5 nm within voids created during the reaction in the grain interior. For the present study, two redox cycles were performed, and the steps of the cycles are herein referred to as reduction 1, oxidation 1, reduction 2, and oxidation 2. In order to characterize the oxidation kinetics, additional times of 0.5, 5, and 10 h were performed for specimens in the oxidation 1 step.

Optical characterization of cross-sectioned and polished pellets was conducted with a low power optical microscope. The extent of the reaction front was quantified by averaging 20 measurements of the depth from the top and bottom surfaces of the pellets. The reaction rate constant and kinetic information were extracted by plotting the squared extent of reaction versus time.

Electron microscopy characterization was performed on specimens prepared by focused ion beam (FIB) milling (FEI, Helios Nanolab 600i) with transition electron microscopy (TEM, Phillips (FEI), CM200) at 200 kV accelerating voltage to show general features of reduction 1 and oxidation 2 microstructures.

AC susceptibility measurements were collected from ~100 to 200 mg of material removed from the pellet with super-conducting

* Corresponding author.
E-mail address: reimanis@mines.edu (I.E. Reimanis).

http://dx.doi.org/10.1016/j.scriptamat.2015.09.025
1359-6462/

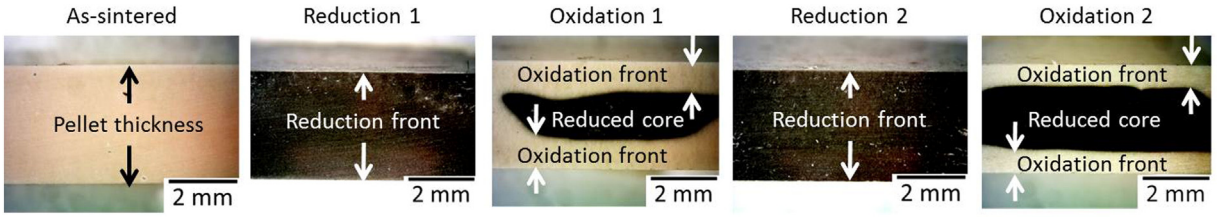

Fig. 1. Optical images showing cross-sections of as-sintered, reduction 1, oxidation 1, reduction 2, and oxidation 2 pellets. Oxidation 1 and 2 pellets contain a reduced core.

Table 1
Summary of the total Ni^0 measured in pellet sections from each redox step.

	Reduction 1	Oxidation 1	Reduction 2	Oxidation 2
Total Ni^0 (%)	43	4	66	24

quantum interference device (SQUID) magnetometry (Quantum Design, MPMS-7) set to an AC drive field of 7 Hz, AC drive amplitude of 100 μT, and zero DC field while scanning temperature from 1.8 to 250 K. The sample of pellet was carefully sectioned so that it represents the entire pellet cross-section. DC susceptibility measurements were also collected by sweeping the field from 1 T to −5 mT at 100 K to obtain a value of magnetic saturation which was used to calculate the percent of reduction using a well-established technique [24].

Optical images of the pellets shown in Fig. 1 depict the color change and extent of reaction. The as-sintered pellet is tan. Reduction 1 turns the entire pellet thickness black. In oxidation 1, the extent of the oxidation front is partial, resulting in a tan coloration, but leaves a black reduced core. The tan coloration of the oxidation 1 pellet is a lighter tint than the as-sintered pellet. Reduction 2 returns the entire pellet thickness to black. In oxidation 2, the extent of the oxidation front is partial, resulting in a green coloration, but leaves a black reduced core. The color changes (tan, black, and green) are the result of changing states of nickel [28]. Tan is due to the substitution of Ni^{2+} on Zr^{4+} sites, black is due to Ni^0 particles, and green is due to NiO. The green color after the second

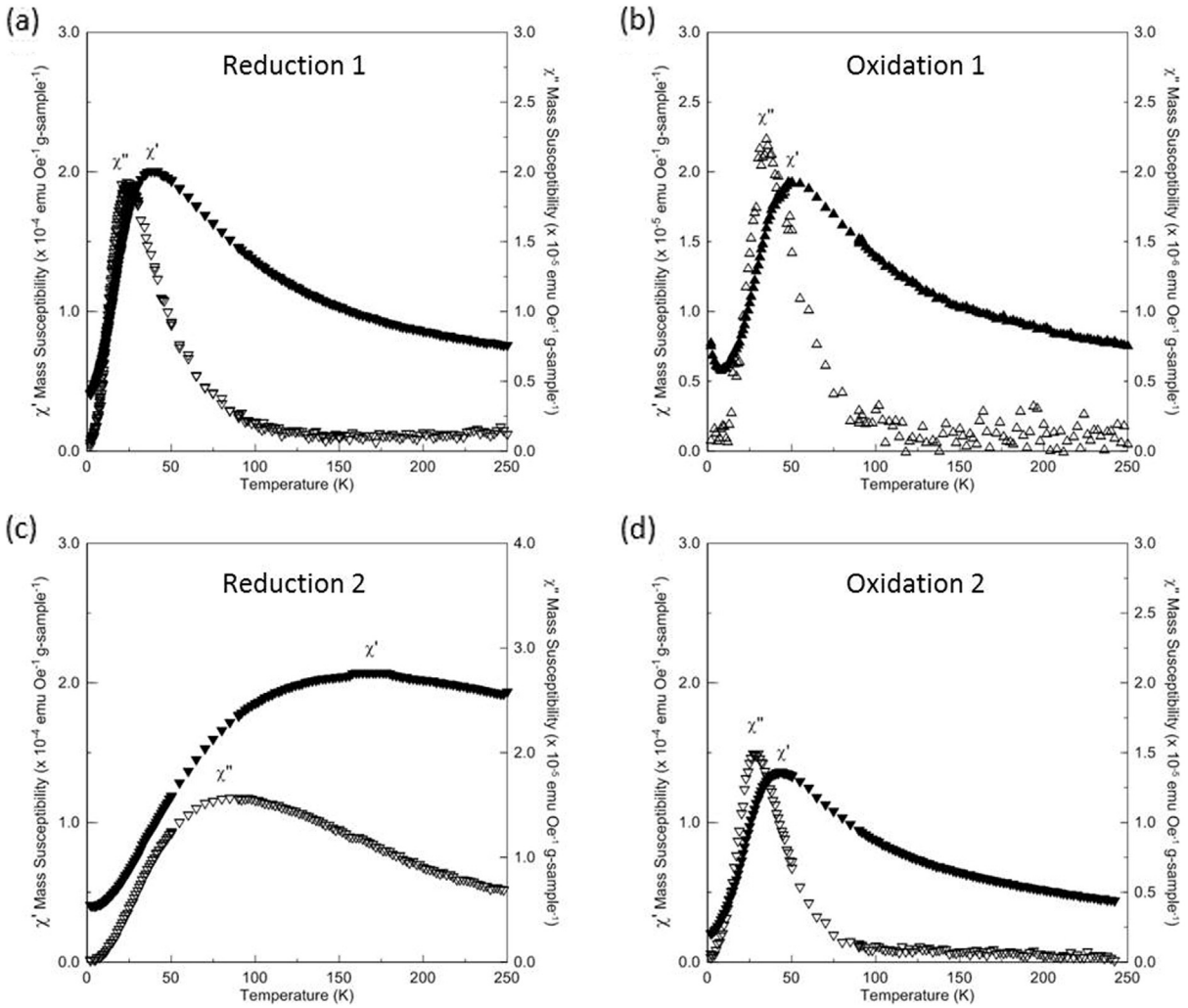

Fig. 2. Plots of AC susceptibility showing the real χ' and imaginary χ'' components for (a) reduction 1, (b) oxidation 1, (c) reduction 2, and (d) oxidation 2. The temperature for which the peak in χ' occurs corresponds to particle size. The growth of Ni^0 particles from reduction 1 to 2 is observed by the peak shift to higher temperature. The peak in oxidation 1 and 2 is equivalent to reduction 1, and indicates that the size of superparamagnetic Ni^0 particles in the reduced core volume is stable after redox cycling.

Please cite this article as: A. Morrissey, et al., Scripta Materialia (2015), http://dx.doi.org/10.1016/j.scriptamat.2015.09.025